HHS Public Access

Author manuscript

Org Biomol Chem. Author manuscript; available in PMC 2022 July 21.

Published in final edited form as:

Org Biomol Chem. 2021 July 21; 19(28): 6237–6243. doi:10.1039/d1ob00705j.

Cytidine Deaminase Can Deaminate Fused Pyrimidine Ribonucleosides

Paul T. Ludford III[a], **Yao Li**[a], **Shenghua Yang**[a], **Yitzhak Tor**[a]

[a]Department of Chemistry and Biochemistry, University of California, San Diego, 9500 Gilman Drive, La Jolla, CA 92093–0358 (USA)

Abstract

The tolerance of Cytidine Deaminase (CDA) to expanded heterocycles is explored via three fluorescent cytidine analogues, where the pyrimidine core is fused to three distinct five-membered heterocycles at the 5/6 positions. The reaction between CDA and each analogue is followed by absorption and emission spectroscopy, revealing shorter reaction times for all analogues than the native substrate. Pseudo-first order and Michaelis-Menten kinetic analyses provide insight into the enzymatic deamination reactions and assist in drawing comparison to established structure activity relationships. Finally, inhibitor screening modalities are created for each analogue and validated with Zebularine and tetrahydrouridine, two known CDA inhibitors.

Graphical Abstract

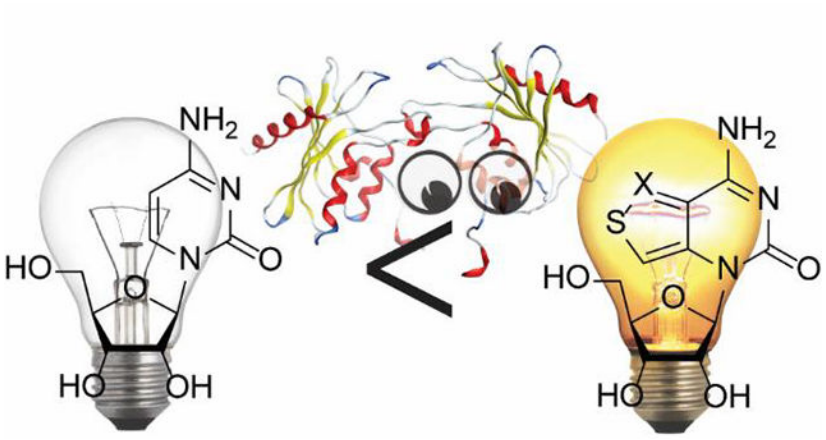

Cytidine Deaminase effectively deaminates three emissive fused cytidine analogues and the reactions can be monitored in real time by fluorescence.

ytor@ucsd.edu.

Author Contributions

Paul T. Ludford III: Data Curation, Formal Analysis, Investigation, Methodology, Software, Validation, Visualization, Writing – Original Draft; Yao Li: Data Curation, Formal Analysis, Investigation, Methodology; Shenghua Yang: Investigation; Yitzhak Tor: Conceptualization, Funding Acquisition, Project Administration, Resources, Supervision, Writing – Review and Editing.

Conflicts of interest

There are no conflicts to declare.

Electronic Supplementary Information (ESI) available: [details of any supplementary information available should be included here]. See DOI: 10.1039/d1ob00705j

Introduction

Cytidine deaminase (CDA) is a key enzyme of the pyrimidine salvage pathway that deaminates cytidine and 2'-deoxycytidine to uridine and 2'-deoxyuridine, respectively (Fig. 1a).[1] It has been shown to also deaminate several chemotherapeutic agents, including the anti-cancer agents cytarabine, gemcitabine and 5'-azadeoxycytidine, thus diminishing their potency.[2–5] Inhibitors of CDA are thus highly sought after for co-administration and mitigation of this detrimental process.[1]

Since deamination involves a nucleophilic attack at the C4 position by a Zn-activated water molecule,[6–8] a common inhibition strategy is to employ transition state analogues, which mimic the tetrahedral intermediate formed.[8–14] Three such inhibitors are diazepinone riboside, phosphapyrimidine riboside, and tetrahydrouridine (THU) (Fig. 1b).[13,15–17] Separate from this approach, zebularine, a cytidine analogue, has been found to be a potent inhibitor as well (Fig. 1b).[16–17] Of these, THU is the only one to have been co-administered with the previously mentioned chemotherapeutic agents.[2–5]

In the search for new inhibitors and substrates, several approaches have been used to monitor CDA activity. These include a colorimetric assay that monitors ammonia production,[18] assays using high performance liquid chromatography to monitor cytidine and uridine concentrations,[19–20] and spectrophotometric assays monitoring changes in absorption spectra.[1,21–22] These assays suffer from lengthy time windows and potential interference by the inhibitors or the protein. As such they are fundamentally unfit for real-time and high throughput operations.

In light of the emerging role of CDA in human disease,[23] the search for new inhibitors of CDA will likely continue, and new rapid methods of monitoring CDA activity and its substrate/inhibitor tolerance are needed. While numerous fluorescent C analogues have been described, to the best of our knowledge, there are none reported that undergo deamination by CDA.[24] That CDA binds the bulkier 7-member ring of Diazepinone riboside suggests the binding pocket might be roomier than previously thought.[8,17] Larger two ring heterocycles, such as purine-related analogues, might therefore be amenable to deamination and augment this repertoire. We therefore set out to explore expanded fluorescent C heterocycles and their CDA tolerance as substrates and potential tools for studying the enzyme and its inhibition.

In recent advances by Shin et al. and Rovira et al., two fluorescent fused cytidine and uridine analogues have been reported (Fig. 1a; ^{tz}**C** and th**C**).[25–27] These fluorescent ribonucleosides absorb above 300 nm and emit in the visible spectrum.[25–27] The emission range and maxima of each C and U analogue pair is distinct, providing a plethora of wavelengths with which to monitor their interconversions. In addition, the spectra are sufficiently red-shifted to minimize potential background signals from proteins and canonical pyrimidine-based inhibitors. We hypothesized that these analogues may thus provide a simple pathway for monitoring CDA activity using fluorescence spectroscopy.

Herein we report three new emissive substrates of CDA and exploit them to provide insight into the enzyme pocket and for fabricating three screening assays. This is facilitated first by

supplementing our previously reported emissive C analogs[25–27] and synthesizing a third fluorescent ribonucleoside analogue pair, ^{mth}**C** and ^{mth}**U** (Fig. 1a). We then monitor the reactions through absorption and emission spectroscopy and compare the reaction rates to establish a structure activity relationship. Finally, we demonstrate the utility of these newfound substrates by assembling a screening assay template with each substrate and validating them using zebularine and THU as model inhibitors.

Results

Synthesis and Photophysical Analysis of ^{mth}C and ^{mth}U

The synthesis of ^{tz}**C** and th**C**, as well as ^{tz}**U** and th**U**, have been reported.[25–27] The pathway to ^{mth}**C** and ^{mth}**U** began with a Michael addition of methyl thioglycolate to methyl crotonate (Scheme 1). The resulting thioether was cyclized under Claisen condensation conditions to yield **1**.[28] Hydroxylamine was added to **1** to yield an oxime, which was subsequently treated with HCl in ether, yielding **2** as a precipitate.[28] Compound **2** was treated with potassium cyanate under mildly acidic conditions to produce the urea **3**.[28] Compound **3** was then cyclized to the nucleobase **4** with sodium methoxide,[28] which was treated with *N,O*-bis(trimethylsilyl)acetamide and then glycosylated with a benzoyl protected ribose precursor in the presence TMS triflate to give the fully protected ^{mth}**U** (**5**).[28] The reaction produced only one diastereomer and crystal structure determination confirmed the proposed structure, revealing the desired beta anomeric configuration (Scheme 1). A portion of nucleoside **5** was deprotected with methanolic ammonia to provide ^{mth}**U**.[28] The remaining was converted to ^{mth}**C** via **6**, by treatment with phosphoryl chloride and triazole in pyridine, followed by ammonolysis in methanolic ammonia (Scheme 1).[28]

Absorption spectra of ^{mth}**C** and ^{mth}**U** were taken in water, displaying maxima at 323 and 306 nm, and extinction coefficients of 3350 and 2550 $M^{-1}cm^{-1}$, respectively. Excitation at these maxima yielded visible emission, with emission maxima at 455 and 427 nm and quantum yields (determined with reference to 2-aminopurine in water) of 0.24 and 0.30, respectively. The resulting Stokes shifts calculated from the absorption and emission maxima were 8930 and 9260 cm^{-1} for ^{mth}**C** and ^{mth}**U**, respectively.

Reactions of Cytidine Analogues With CDA

To determine whether CDA accepted ^{tz}**C**, th**C** and ^{mth}**C** as substrates, HPLC analysis of their enzymatic deamination reactions was performed and compared to the reaction of the native substrate. Chromatograms taken after 60 minutes confirmed complete conversion to uridine or the corresponding U analogue (Fig. S1–4). The reactions were then monitored via changes in absorbance (Fig. 2a–c). Initially, steady state traces were taken various time points during the reaction revealing isosbestic points for ^{tz}**C** and ^{tz}**U**, th**C** and th**U**, and ^{mth}**C** and ^{mth}**U** at 293, 292, and 305 nm respectively. For each analogue pair, the absorption intensity decreased and blue-shifted as the reaction progressed (Fig. 2a–c). The reactions were further monitored by changes in emission upon excitation at the respective isosbestic point (Fig. 2d–f). Steady state traces were taken at various time points over 30 minutes. As ^{tz}**C** converted to ^{tz}**U**, emission intensity decreased and blue-shifted (Fig. 2d). For the conversion of th**C** to th**U**, emission intensity slightly increased and slightly blue shifted

revealing an isoemissive point at 430 nm (Fig. 2e). As ^{mth}**C** converted to ^{mth}**U**, emission intensity increased and blue-shifted (Fig. 2f). The absorption of ^{tz}**C**, th**C**, and ^{mth}**C** reactions with CDA was then monitored at 340, 330, and 330 nm respectively (Fig. 3a,c). Finally, the emission of ^{tz}**C**, th**C**, and ^{mth}**C** reactions with CDA were recorded at 408, 400, and 427 nm, respectively, upon excitation at the corresponding isosbestic point (Fig. 3b,d).

Analysis of the Reactions of Cytidine Analogues With CDA

The data from the aforementioned reactions monitored by absorption and emission were analyzed using two kinetic models, a pseudo-first order model (Eq. 1–2) and a set of differential equations based on Michaelis-Menten kinetics (Eq. 3–6). The pseudo-first order model fits to the absorption curves revealed k_{app} values of 3.1 ± 0.1, 3.3 ± 0.1, 7.2 ± 0.2, and 6.1 ± 0.2 s^{-1} and $t_{1/2}$ values of 220 ± 12, 210 ± 16, 92 ± 5, and 110 ± 2 s for **C**, ^{tz}**C**, th**C**, and ^{mth}**C**, respectively. The pseudo-first order model fits to the emission curves revealed k_{app} values of 4.1 ± 0.1, 7.4 ± 0.1, and 5.7 ± 0.1 s^{-1} and $t_{1/2}$ values of 170 ± 10, 94 ± 2, and 120 ± 8 s for ^{tz}**C**, th**C**, and ^{mth}**C**, respectively.

$$\left[S\right] = [S]_0 e^{-k_{app}t} \tag{1}$$

$$[P] = [S]_0\left(1 - e^{-k_{app}t}\right) \tag{2}$$

$$\frac{d[S]}{dt} = -k_1[E][S] + k_{-1}\left[ES\right] \tag{3}$$

$$\frac{d[E]}{dt} = -k_1[E][S] + k_{-1}[ES] + k_2\left[ES\right] \tag{4}$$

$$\frac{d[ES]}{dt} = k_1[E][S] - k_{-1}[ES] - k_2\left[ES\right] \tag{5}$$

$$\frac{d[P]}{dt} = k_2\left[ES\right] \tag{6}$$

$$K_I = \frac{IC_{50}}{1 + \frac{[S]}{K_M}} \tag{7}$$

Analysis of the absorption curves via the Michaelis-Menten differential equations revealed k_1 values of 0.91 ± 0.42, 1.04 ± 0.01, 1.01 ± 0.47, and 0.75 ± 0.16 μM^{-1} s^{-1} and k_2 values of 3.2 ± 2.1, 3.2 ± 0.3, 34 ± 7.2, and 56 ± 5.9 s^{-1} for **C**, ^{tz}**C**, th**C** and ^{mth}**C,** respectively. Analysis of the emission curves via the same method revealed k_1 values of 1.06 ± 0.32, 0.95 ± 0.14 and 0.71 ± 0.18 μM^{-1} s^{-1} and k_2 values of 4.6 ± 1.3, 46 ± 5.3, and 45 ± 2.3 s^{-1} for ^{tz}**C**, th**C** and ^{mth}**C,** respectively. k_{-1} values were assumed to be 10% of k_1 values. K_M values

calculated from the k_1, k_{-1}, and k_2 values of the absorption curve fits were 3.6, 3.1, 34, and 75 μM for **C**, ^{tz}**C**, th**C**, and ^{mth}**C,** respectively. The K_M of **C** previously reported for the Q27/A70 variant of CDA, which was used in this work, was 17.6 μM. K_M values calculated from the k_1, k_{-1}, and k_2 values obtained from the emission curve fits were 4.4, 49, and 63 μM for ^{tz}**C**, th**C** and ^{mth}**C,** respectively.

Inhibition by Zebularine and THU

Testing the potency of zebularine as a CDA inhibitor using ^{tz}**C**, th**C** and ^{mth}**C** as C surrogates revealed IC_{50} values of 5.0 ± 0.4, 2.7 ± 0.2, and 1.5 ± 0.1 μM, respectively (Table 2). Using the Cheng-Prusoff equation (Eq. 7), K_I values were calculated to be 1.5 ± 0.1, 2.2 ± 0.1, and 1.3 ± 0.1 μM, respectively (Table 2). Similarly, evaluating THU as an inhibitor employing ^{tz}**C**, th**C**, and ^{mth}**C** revealed IC_{50} values of 3.1 ± 0.5, 1.7 ± 0.3, and 0.61 ± 0.11 μM, respectively (Table 2). K_I values were found to be 0.95 ± 0.16, 1.4 ± 0.2, and 0.53 ± 0.10 μM, respectively. Reassessing zebularine using ^{mth}**C** as the emissive surrogate in the presence of 100 μM adenosine revealed IC_{50} and K_I values of 2.34 ± 0.59 and 2.02 ± 0.51 μM, respectively.

Discussion

Over the years, highly isomorphic fluorescent ribonucleosides have provided insight into enzyme kinetics and substrate specificity.[29–33] The diverse cellular pathways these enzymes take range anywhere from immune response and signalling to purine degradation and general metabolism.[29–33] In the case of adenosine deaminase (ADA), comparing two adenosine analogues as substrates illustrated the importance of N7 on deamination kinetics.[26,27,29,32] We took this case as inspiration for further exploring other enzymes including cytidine deaminase. We suspected that, as in the case of ADA, synthetic cytidine analogues might be able to provide indirect insight into CDA substrate scope. We thus explored the ability of CDA to deaminate increasingly perturbed C analogues, with distinct levels of steric bulk and heteroatom composition, ranging from ^{tz}**C**, th**C**, to ^{mth}**C** (Fig. 1a). We already had previously synthesized ^{tz}**C** and th**C**, but ^{mth}**C** had yet to be reported so we began by developing a synthetic route to it.

Synthesis of ^{mth}**C** started with cheap, commercially available starting materials methyl thioglycolate and methyl crotonate and was completed over 7 steps (Scheme 1). The corresponding U analogue ^{mth}**U**, the potential product of a reaction of ^{mth}**C** with CDA, was synthesized so that it could be used as a reference to confirm successful deamination by CDA (Scheme 1). In anticipation of the spectral changes that would be observed during a reaction of ^{mth}**C** with CDA, we compared the absorption and emission spectra of ^{mth}**C** and ^{mth}**U**. Extinction coefficients, Stokes shifts, and quantum yields were calculated indicating decreases in absorption at wavelengths above 305 nm, and increases in emission intensity at wavelengths between 360 and 470 nm would occur if ^{mth}**C** was converted to ^{mth}**U**.[28]

With the new and previously reported analogues in hand, we incubated cytidine and each C analogue with CDA for 60 minutes. The reactions were HPLC analyzed, confirming all three substrates were deaminated to completion (Fig. S1–4).[28] To explore whether the unique spectral features of the analogues could be used to monitor the deamination reactions, we

first monitored the steady state absorption spectra of a reaction of CDA with each C analogue over 30 minutes (Fig. 2a–c). The spectra revealed isosbestic points of 293 nm for ^{tz}**C** and ^{tz}**U**, 292 nm for th**C** and th**U**, and 305 nm for ^{mth}**C** and ^{mth}**U** (Fig. 2a–c). Steady state emission spectra were then taken at the same time points during the reaction by exciting at the respective isoabsorptive wavelengths (Fig. 2d–f). The resulting spectra indicated a range of wavelengths from the near UV to the visible spectrum with which to spectroscopically observe their enzymatic interconversion (Fig. 2). We chose to monitor the reaction of cytidine, ^{tz}**C**, th**C**, and ^{mth}**C** with CDA via absorption at 260 nm, 340 nm, 330 nm, and 330 nm respectively (Fig. 3a,c). We also chose to monitor the reaction of ^{tz}**C**, th**C**, and ^{mth}**C** via emission at 408 nm upon excitation at 293 nm, 400 nm upon excitation at 292 nm, and 427 nm upon excitation at 305 nm respectively (Fig. 3b,d). The reaction times to completion of all three C analogues were found to be shorter than cytidine in both absorption and emission (Table 1).

To quantify our observations, curves assuming pseudo-first order conditions were fit to the data yielding k_{app} values (Eqs. 1–2, Table 1). The k_{app} values were converted to $t_{1/2}$ values for further comparison (Table 1). The reaction $t_{1/2}$ value for ^{tz}**C** was found to be slightly shorter than C while the $t_{1/2}$ values for th**C** and ^{mth}**C** were found to be two- to three-fold shorter with th**C** being the shortest (Table 1). The k_{app} and $t_{1/2}$ values determined by curve fitting the observed changes in absorption and emission were found to be in good agreement with each other (Fig. 3a,b, Table 1). Intriguingly, the reaction rates suggested the addition of a thiophene ring off of the 5 and 6 positions of the pyrimidine ring improved deamination kinetics by CDA.

To further clarify these observations, a set of differential equations corresponding to the Michaelis-Menten kinetics were solved setting initial concentrations to those used in the experiments to yield time dependent substrate and product concentration curves.[34–36] Those curves were fitted to the experimental data and optimized by maximizing R^2, yielding k_1, k_2, and K_M values (Eqs. 3–6, Fig. 3c,d, Table 1). While perhaps less accurate than a thorough Michaelis-Menten analyses, this streamlined approach was taken as our goal was to only compare several related substrates to one another and gain insight into their interactions with the enzyme. k_{-1} values below 10% of k_1 values had minimal effect on R^2 (varying less than 0.0001). K_M values were only slightly affected at this range (3.3% at most), thus we restricted k_{-1} values to 10% of k_1 values, effectively setting them as an upper limit to what they could be. K_M values of CDA with various substrates have been previously reported indicating the enzyme adheres to Michaelis-Menten kinetics.[1,2,6,12,17,18,20–23] The model revealed a slightly larger binding rate constant (k_1) for ^{tz}**C** and th**C** when compared to cytidine, suggesting the fusion of a five-membered isothiazole or thiophene ring improved binding. The slightly smaller binding rate constant for ^{mth}**C** indicated the bulky methyl group diminishes binding, but not detrimentally, suggesting some tolerance for steric perturbation. The model further showed the deamination and unbinding rate constant (k_2) for th**C** and ^{mth}**C** was faster than cytidine, but about the same for ^{tz}**C** as compared to cytidine (Table 1). This indicated the shorter $t_{1/2}$ observed for ^{mth}**C** was dominated by the deamination rate rather than binding. This further confirmed the expansion of the ring system in cytidine could potentially improve substrate reception by the enzyme.

With a number of new substrates to monitor CDA activity effectively and in real time, we chose two known inhibitors, zebularine and THU, to validate these emissive nucleosides as tools for screening assays. Reactions of each C analogue with CDA were monitored via emission under the same conditions as described above, but with varying concentrations of either inhibitor (Fig. 4a,b). A selected time point for each reaction was compared to a reference reaction without inhibitor and plotted against inhibitor concentration (Fig. 4c,d). IC_{50} values were calculated from Hill curves fit to the resulting plots (Fig. 4c,d). The IC_{50} values were then converted to K_I values via the Cheng-Prusoff equation (Eq. 7, Table 2). The K_I values of zebularine and THU show slight variance between the three substrates used. While its origin is unclear at present, we note that Laliberte et al. have also reported discrepancies in K_I values for zebularine and THU depending on the substrates used.[17] In addition, zebularine was analyzed in the presence of 100 μM adenosine with ^{mth}**C** by the same method as described without adenosine (Fig. 4c). The IC_{50} and K_I values resulting from the analysis with 100 μM adenosine are 2.34 ± 0.59 and 2.02 ± 0.51 μM, respectively, in good agreement with the values calculated without adenosine (Table 2). The consistency in IC_{50} and K_i values confirmed that each C analogue was an effective alternative for characterizing inhibitors of CDA. Furthermore, the similarity of the IC_{50} and K_I values obtained with and without excess adenosine using ^{mth}**C** to monitor CDA activity indicated that background signal from similar molecules was less of a factor.

Conclusions

To explore the binding pocket of CDA, a new fluorescent C and U analogue pair, ^{mth}**C** and ^{mth}**U**, was synthesized (Scheme 1). The absorption and emission spectra were analyzed yielding extinction coefficients, Stokes shifts, and emission quantum yields. Upon reacting ^{mth}**C** and two previously synthesized C analogues, ^{tz}**C** and th**C**, with CDA we discovered that all three serve as viable substrates and, in fact, have shorter reaction half-lives than the native cytidine (Table 1). This confirmed our hypothesis that fusing additional aromatic rings onto the pyrimidine core may retain substrate viability by CDA. Further analysis indicated that the thieno- and isothiazolo-based analogs improved binding affinity and accelerated deamination rates while a methyl substitution onto the thiophene slightly diminished binding affinity (Table 1). We were also able to use ^{tz}**C**, th**C**, and ^{mth}**C** to establish three new templates for spectroscopy-based screening assays with zebularine and THU as model inhibitors (Fig. 4). As all three C and U analogues have red shifted absorption and emission spectra relative to the native cytidine and uridine, we submit these may be attractive alternatives for monitoring CDA activity and its inhibition as a foundation of screening campaigns.

Supplementary Material

Refer to Web version on PubMed Central for supplementary material.

Acknowledgements

We thank the National Institutes of Health for generous support (through grant GM 069773) and the Chemistry & Biochemistry MS Facility. We thank Dr. Milan Gembicky the UCSD X-ray Crystallography Facility for determining the crystal structure. We thank Dr. Anthony Mrse and the UCSD NMR Facility for assistance.

Notes and references

1. Micozzi D, Carpi FM, Pucciarelli S, Polzonetti V, Polidori P, Vilar S, Williams B, Costanzi S and Vincenzetti S, Int. J. Biol. Macromol, 2014, 63, 64–74. [PubMed: 24183806]
2. Voorde JV, Vervaeke P, Liekens S and Balzarini J, FEBS Open Bio 2015, 5, 634–639.
3. Bjånes TK, Jordheim LP, Schjøtt J, Kamceva T, Cros-Perrial E, Langer A, de Garibay GR, Kotopoulis S, McCormack E and Riedel B, Drug Metab. Dispos, 2020, 48 (3), 153–158. [PubMed: 31871136]
4. Bowen C, Wang S and Licea-Perez H, J. Chromatogr. B Anal. Technol. Biomed. Life Sci, 2009, 877 (22), 2123–2129.
5. Lavelle D, Vaitkus K, Ling Y, Ruiz MA, Mahfouz R, Ng KP, Negrotto S, Smith N, Terse P, Engelke KJ, Covey J, Chan KK, DeSimone J and Saunthararajah Y, Blood, 2012, 119 (5), 1240–1247. [PubMed: 22160381]
6. Cambi A, Vincenzetti S, Neuhard J, Costanzi S, Natalini P and Vita A, Protein Eng, 1998, 11 (1), 59–63. [PubMed: 9579661]
7. Teh AH, Kimura M, Yamamoto M, Tanaka N, Yamaguchi I and Kumasaka T, Biochemistry, 2006, 45 (25), 7825–7833. [PubMed: 16784234]
8. Chung SJ, Fromme JC and Verdine GL, J. Med. Chem, 2005, 48 (3), 658–660. [PubMed: 15689149]
9. Liu PS, Marquez VE, Kelley JA and Driscoll JS, J. Org. Chem, 1980, 45 (25), 5225–5227.
10. Marquez VE, Liu PS, Kelley JA, Driscoll JS and McCormack JJ, J. Med. Chem, 1980, 23 (7), 713–715. [PubMed: 7401098]
11. Kim CH, Marquez VE, Mao DT, Haines DR and McCormack JJ, J. Med. Chem, 1986, 29 (8), 1374–1380. [PubMed: 3735306]
12. McCormack JJ, Marquez VE, Liu PS, Vistica DT and Driscoll JS, Biochem. Pharmacol, 1980, 29 (5), 830–832. [PubMed: 20227965]
13. Ashley GW and Bartlett PA, J. of Biological Chemistry, 1984, 259 (21), 13621–13627.
14. Frick L, Yang C, Marquez VE and Wolfenden R, Biochemistry, 1989, 28 (24), 9423–9430. [PubMed: 2692708]
15. Funamizu N, Lacy CR, Fujita K, Furukawa K, Misawa T, Yanaga K and Manome Y, PLoS One, 2012, 7 (5), e37424. [PubMed: 22616006]
16. Marquez VE, Barchi JJ, Kelley JA, Rao KVR, Agbaria R, Ben-Kasus T, Cheng JC, Yoo CB and Jones PA, Nucleosides, Nucleotides and Nucleic Acids, 2005, 24 (5–7), 305–318.
17. Laliberte J, Marquez VE and Momparler RL, Cancer Chemotherapy and Pharmacology, 1992, 30, 7–11. [PubMed: 1375134]
18. Okamura T and Kigasawa K, Prenat. Diagn, 1994, 14 (3), 213–218. [PubMed: 8052571]
19. Sherwood RA, Biomed. Chromatogr, 1991, 5 (6), 235–239. [PubMed: 1760590]
20. Dutta PK, Shanley MS and O'Donovan GA, J. Chromatogr. A, 1990, 512 (C), 395–401.
21. Chabner BA, Drake JC and Johns DG, Biochem. Pharmacol, 1973, 22 (21), 2763–2765. [PubMed: 4128550]
22. Wentworth DF and Wolfenden R, Biochemistry, 1975, 14 (23), 5099–5105. [PubMed: 53069]
23. Frances A and Cordelier P, Mol. Therapy, 2020, 28 (2), 357–366.
24. Sinkeldam RW, Greco NJ and Tor Y, Chem. Rev, 2010, 110, 2579–2619. [PubMed: 20205430]
25. Shin D, Sinkeldam RW and Tor Y, J. Am. Chem. Soc, 2011, 133 (38), 14912–14915. [PubMed: 21866967]
26. Rovira AR, Fin A and Tor Y, J. Am. Chem. Soc, 2015, 137 (46), 14602–14605. [PubMed: 26523462]
27. Rovira AR, Fin A and Tor Y, Chem. Sci, 2017, 8, 2983–2993. [PubMed: 28451365]
28. See supporting information.
29. Sinkeldam RW, McCoy LS, Shin D and Tor Y, Angew. Chem. Int. Ed, 2013, 52, 14026–14030.
30. Rovira AR, Fin A and Tor Y, J. Am. Chem. Soc, 2017, 139, 15556–15559. [PubMed: 29043790]
31. Hallé F, Fin A, Rovira AR and Tor Y, Angew. Chem. Int. Ed, 2017, 57, 1087–1090.

32. Ludford III PT, Rovira AR, Fin A and Tor Y, ChemBioChem, 2019, 20, 718–726. [PubMed: 30566279]
33. Li Y, Ludford III PT, Fin A, Rovira AR and Tor Y, Chem. Eur. J, 2020, 26, 6076–6084. [PubMed: 32157755]
34. Ashyraliyev M, Fomekong-Nanfack Y, Kaandorp JA, and Blom JG, FEBS Journal, 2009, 276, 886–902.
35. Kutalik Z, Cho K-H, Wolkenhauer O, BioSystems, 2004, 75, 43–55. [PubMed: 15245803]
36. Hoops S, Hontecillas R, Abedi V, Leber A, Philipson C, Carbo A, and Bassaganya-Riera J, in Computational Immunology: Models and Tools, ed. Bassaganya-Riera J, Academic Press, 2016, ch. 5, 63–78.

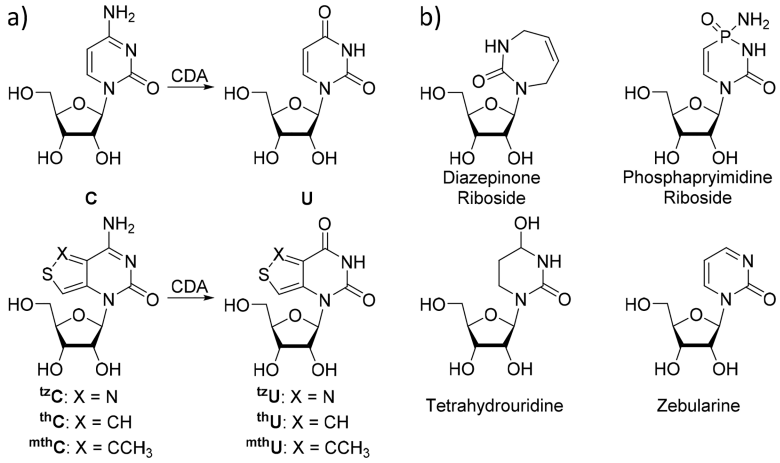

Figure 1.

a) Top: Enzymatic deamination of cytidine to uridine by CDA; Bottom: Enzymatic deamination of ^{tz}**C**, th**C**, and ^{mth}**C** to ^{tz}**U**, th**U**, and ^{mth}**U**, respectively; b) CDA Inhibitors diazepinone riboside, phospharpyrimidine riboside, tetrahydrouridine, and zebularine.

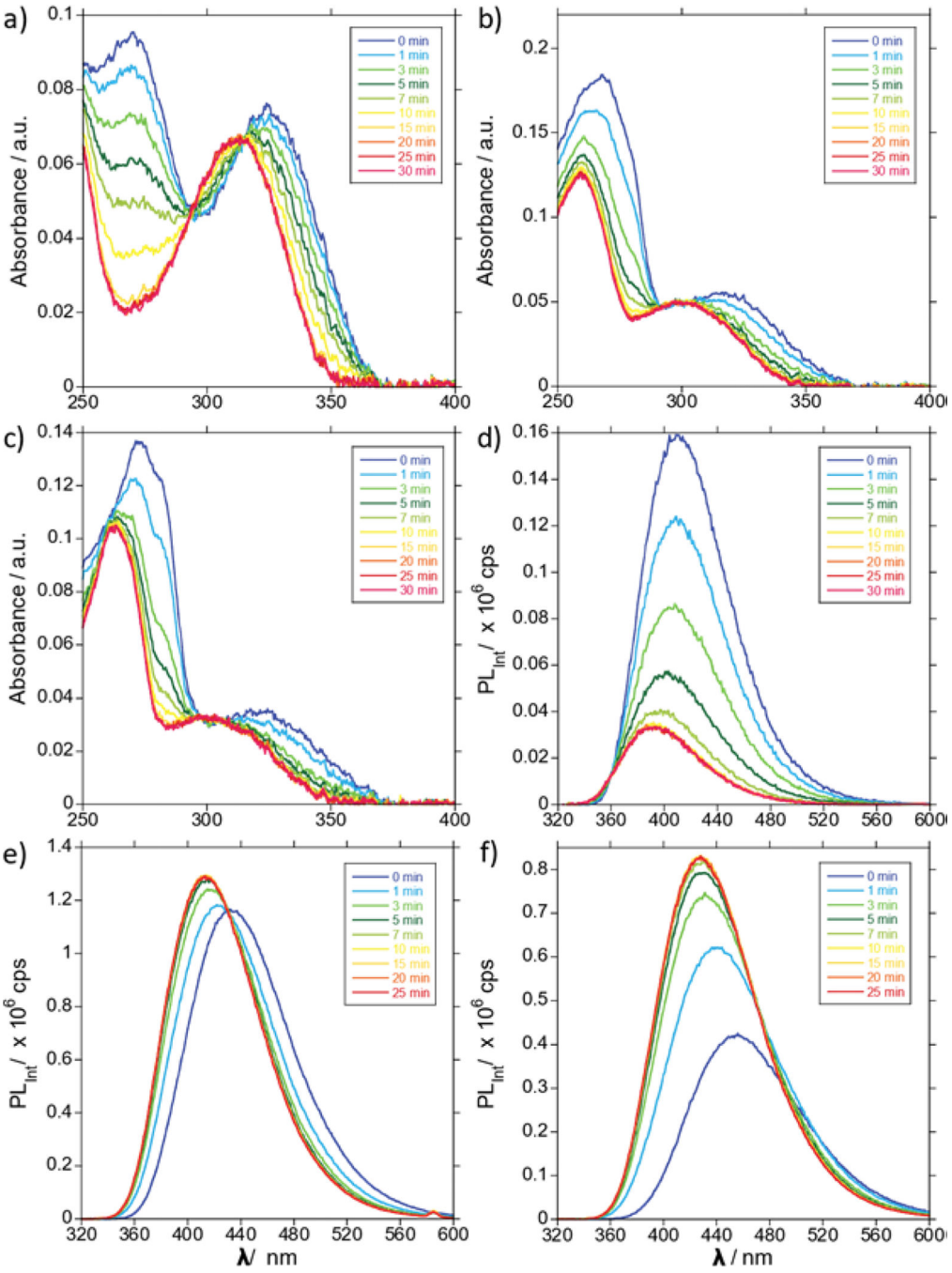

Figure 2.

Steady state absorption traces of (a) ^{tz}**C**, (b) th**C**, and (c) ^{mth}**C** CDA-mediated conversion to ^{tz}**U**, th**U**, and ^{mth}**U** respectively, over a time range from 0 to 30 min; Steady state emission traces of (d) ^{tz}**C**, (e) th**C**, and (f) ^{mth}**C** CDA-mediated conversion to ^{tz}**U**, th**U**, and ^{mth}**U** respectively, over a time range from 0 to 30 min.

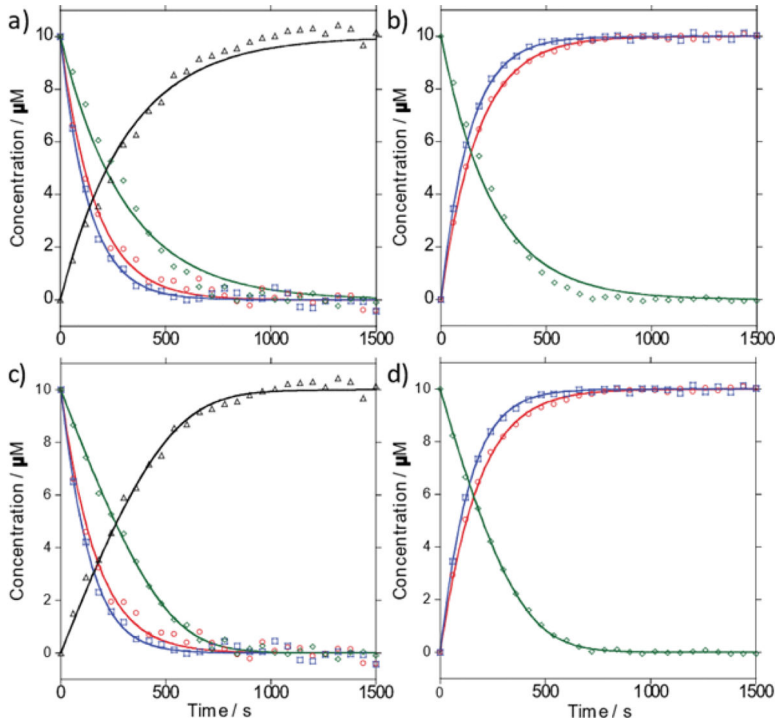

Figure 3.

Enzymatic conversion of **C** (black), ^{tz}**C** (green), th**C** (blue), and ^{mth}**C** (red) to **U**, ^{tz}**U**, th**U**, and ^{mth}**U** by CDA. Reactions were monitored by absorbance (a, c) and emission (b, d) and fit to a first order curve (a, b) or to an integrated Michaelis-Menten set of differential equations (c, d).

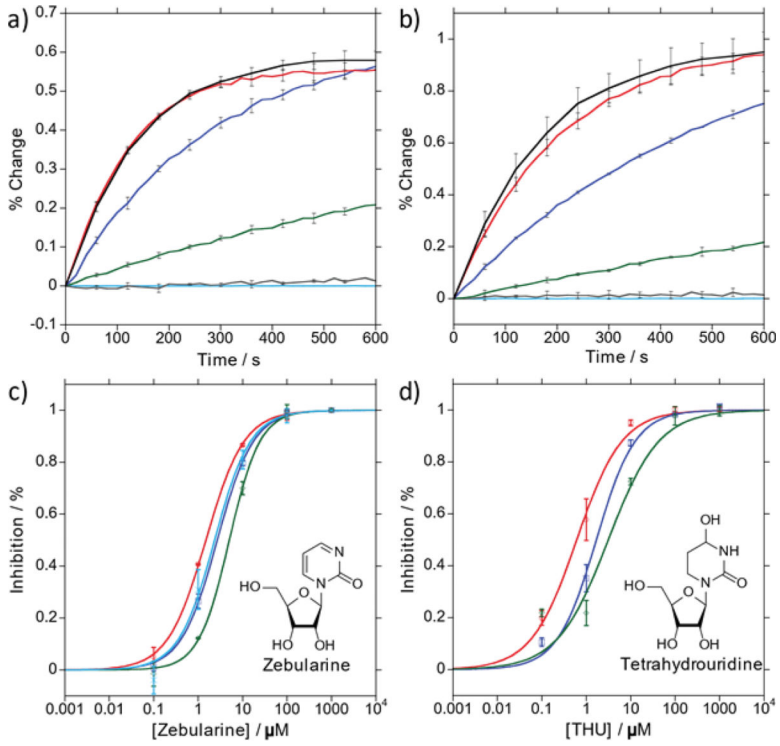

Figure 4.

a, b) Conversion of th**C** to th**U** (a) and ^{mth}**C** to ^{mth}**U** (b) in the presence of various concentrations of Zebularine ([I] = 0 μM (black), 0.1 μM (red), 1 μM (blue), 10 μM (green), 100 μM (grey), 1 M (light blue). c, d) Semi-log plot of % inhibition in decimal form after 4 (th**C**) or 5 (^{tz}**C**, ^{mth}**C**) minutes versus [Zebularine] (c) or [THU] (d) fit to a sigmoidal Hill curve: ^{tz}**C** (green), th**C** (blue), ^{mth}**C** (red), ^{mth}**C** with 100 μM Adenosine (light blue).

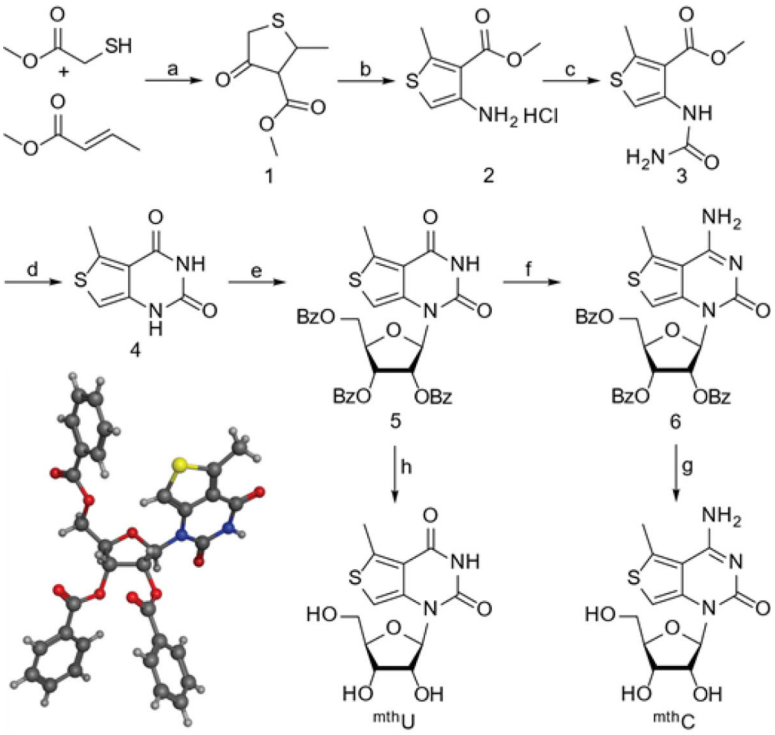

Scheme 1.

Synthetic pathways to ^{mth}**U** and ^{mth}**C**; [a]Reagents and Conditions: (a) i) Piperidine, 50^{o}C, 2 h; ii) NaH (60% in mineral oil), THF, 70^{o}C, overnight, 19% over two steps. (b) i) **1**, $BaCO_3$, hydroxylamine hydrochloride, MeOH, 70^{o}C, overnight; ii) 2M HCl in OEt_2, OEt_2, MeOH, RT, 24 h, 78% over two steps. (c) Potassium cyanate, acetic acid (30%), RT, overnight, 94%. (d) Sodium methoxide, MeOH, RT, 15 h, 91%. (e) *N,O*-bis(trimethylsilyl)acetamide, β-D-ribofuranose 1-acetate 2,4,5-tribenzoate, TMS Triflate, ACN, 85^{o}C, 3 h, 85%. (f) i) Phosphoryl (V) Chloride, 1,2,4-triazole, pyridine, RT, 1 h; ii) Saturated ammonium hydroxide, RT, 3 h, 43% over two steps. (g) Ammonia saturated MeOH, 65^{o}C, overnight, 53%. (h) Ammonia saturated MeOH, 65^{o}C, overnight, 85%. Inset: Crystal structure of **5**.

Table 1.

Reaction Rate Constants for CDA Mediated Deamination.

		Pseudo-First Order			Michaelis-Menten			
		k_{app} (x 10^{-3} s^{-1})	$t_{1/2}$ (s)	R^2	k_1 (μM^{-1} s^{-1})	k_{-1}[a] (s^{-1})	k_2 (s^{-1})	K_M (μM)[b]
Abs	C	3.1 ± 0.1	220 ± 12	0.981	0.91 ± 0.42	0.091	3.2 ± 2.1	3.6
	^{tz}C	3.3 ± 0.1	210 ± 16	0.979	1.04 ± 0.01	0.104	3.2 ± 0.3	3.1
	thC	7.2 ± 0.2	92 ± 5	0.992	1.01 ± 0.47	0.101	34 ± 7.2	34
	^{mth}C	6.1 ± 0.2	110 ± 2	0.987	0.75 ± 0.16	0.075	56 ± 5.9	75
Em	^{tz}C	4.1 ± 0.1	170 ± 10	0.988	1.06 ± 0.32	0.106	4.6 ± 1.3	4.4
	thC	7.4 ± 0.1	94 ± 2	0.999	0.95 ± 0.14	0.095	46 ± 5.3	49
	^{mth}C	5.7 ± 0.1	120 ± 8	0.999	0.71 ± 0.18	0.071	45 ± 2.3	63

*Data are presented as mean ± SD.

[a]Values were assumed to be ≤10% of k_1 values.

[b]Values calculated from k_1, k_{-1}, and k_2.

Table 2.

Experimentally Determined IC_{50} and K_I Values of Zebularine and THU.

	Inh.	IC_{50} (μM)	K_I (μM)	R^2
^{tz}C	Zeb	5.0 ± 0.4	1.5 ± 0.1	0.999
^{th}C	Zeb	2.7 ± 0.2	2.2 ± 0.1	0.999
^{mth}C	Zeb	1.5 ± 0.1	1.3 ± 0.1	0.999
^{tz}C	THU	3.1 ± 0.5	0.95 ± 0.16	0.948
^{th}C	THU	1.7 ± 0.3	1.4 ± 0.2	0.995
^{mth}C	THU	0.61 ± 0.11	0.53 ± 0.10	0.995

*Data are presented as mean ± SD.